The Single Mutation Phe173 → Ala Induces a Molten Globule-like State in Murine Interleukin-6[†]

Jacqueline M. Matthews,[‡,§] Raymond S. Norton,[||] Annet Hammacher,[‡] and Richard J. Simpson*[,‡]

Joint Protein Structure Laboratory, Ludwig Institute for Cancer Research (Melbourne Tumour Biology Branch) and Walter and Eliza Hall Institute of Medical Research, P.O. Box 2008, Royal Melbourne Hospital, Parkville 3050, Victoria, Australia, and Biomolecular Research Institute, 343 Royal Pde, Parkville 3052, Victoria, Australia

Received August 23, 1999; Revised Manuscript Received October 25, 1999

ABSTRACT: A series of three aromatic to alanine mutants of recombinant murine interleukin-6 lacking the 22 N-terminal residues (ΔN22mIL-6) were constructed to investigate the role of these residues in the structure and function of mIL-6. While Y78A and Y97A have activities similar to that of ΔN22mIL-6, F173A lacks biological activity. F173A retains high levels of secondary structure, as determined by far-UV circular dichroism (CD), but has substantially reduced levels of tertiary structure, as determined by near-UV CD and ^{1}H NMR spectroscopy. F173A also binds the hydrophobic dye 1-anilino-8-naphthalenesulfonic acid (ANS) over a range of pH values and exhibits noncooperative equilibrium unfolding (as judged by the noncoincidence of monophasic unfolding transitions monitored by far-UV CD and λ_{max}, with midpoints of unfolding at 2.6 ± 0.1 and 3.5 ± 0.3 M urea, respectively, and the lack of an observable thermal unfolding transition). These are all properties of molten globule states, suggesting that the loss of activity of F173A results from the disruption of the fine structure of the protein, rather than from the loss of a side chain that is important for ligand−receptor interactions. Surprisingly, under some conditions, this loosened conformation is no more susceptible to proteolytic attack than the parent protein. By analogy with human IL-6, Phe173 in ΔN22mIL-6 makes multiple interhelical interactions, the removal of which appear to be sufficient to induce a molten globule-like conformation.

Interleukin-6 (IL-6)[1] is a pleiotropic cytokine that plays a central role in tissue injury and host defense against infection (*1*−*3*). Its dysregulated production is associated with diverse diseases such as rheumatoid arthritis, psoriasis, postmenopausal osteoporosis (*4*), multiple myeloma (*5*), and Kaposi's sarcoma (*6*). A more complete understanding of IL-6 and its signaling mechanisms may lead to the development of therapeutics for the treatment of such diseases.

IL-6 first binds with low affinity to the IL-6 receptor (IL-6R) to form a binary complex which binds with high affinity to gp130, resulting in intracellular signaling (*7*). The soluble IL-6−IL-6R−gp130 complex is hexameric (*8*, *9*), but its topology is not yet known. Both crystal and solution structures of IL-6 have been published recently (*10*, *11*), confirming that it is a four-α-helix bundle with up−up−down−down topology. The crystal structure of the cytokine binding domain of gp130 has also been solved (*12*), but as yet, no reports of structures for the higher complexes of IL-6, IL-6R and gp130 have been published. However, several mutagenic and chimeric studies have resulted in the identification of three separate binding sites on hIL-6 for the IL-6R and gp130 (reviewed in (*3*)).

Techniques such as alanine scanning (*13*, *14*), whereby individual residues or stretches of residues are selectively mutated to alanine throughout most of the protein sequence, are commonly used to identify residues critical for activity. This is because mutation to alanine from any residue (other than glycine) effectively trims the side chain beyond the β-carbon and is considered to be generally nonperturbing, where the only effects on structure occur close to the site of mutation (*15*). However, the effect of mutation on structure is not always predictable, and interpretation of the loss of activity in mutant proteins can be misleading.

In this study, a series of aromatic to alanine mutants of a variant of murine IL-6 which lacks 22 N-terminal residues, ΔN22mIL-6 (*16*), were constructed to determine the role of these residues in the structure and function of mIL-6. The deleted residues of ΔN22mIL-6 are disordered (*10*, *17*−*20*) and can be deleted without the loss of biological function (*16*). Of the aromatic residues that were studied, only Phe173 appears to be biologically significant as mutation to alanine eliminates biological activity.

Although F173A is similar to its parent protein in some respects, more detailed studies reveal that the structure is highly perturbed, with many molten globule-like characteristics. This stresses the need for sufficient structural char-

[†] This work was supported in part by Grant 950824 from the National Health and Medical Research Council of Australia.

* To whom correspondence should be addressed: Ludwig Institute for Cancer Research, P.O. Box 2008, Royal Melbourne Hospital, Parkville 3050, Victoria, Australia. E-mail: Richard.Simpson@ludwig.edu.au. Fax: +61 3 9341 3104.

[‡] Joint Protein Structure Laboratory, Ludwig Institute for Cancer Research and Walter and Eliza Hall Institute of Medical Research.

[§] Current address: Department of Biochemistry, University of Sydney, NSW 2006, Australia.

[||] Biomolecular Research Institute.

[1] Abbreviations: ANS, 1-anilino-8-naphthalenesulfonic acid; CD, circular dichroism; IL-6, interleukin-6; ΔN22mIL-6, N-terminally truncated form of murine IL-6.

10.1021/bi991973i CCC: $19.00
Published on Web 02/04/2000

acterization of proteins that are found to be inactive in mutagenic scans before it can be assumed that the altered residues form part of active or binding sites.

MATERIALS AND METHODS

Construction, Expression, and Purification of ΔN22mIL-6, Y78A, Y97A, and F173A. The generation of ΔN22mIL-6 has been described previously (*16*) Fragments encoding Y78A, Y97A, and F173A were generated by polymerase chain reaction (PCR) using the pUC8-derived plasmid p9HP1B5B12 (encoding mouse IL-6) as a template. Following restriction endonuclease treatment and agarose gel purification, these fragments were used to replace corresponding nonmutated ΔN22mIL-6 fragments for expression in pUC8. All constructs were verified by DNA sequencing using a model 370A DNA sequencer (Applied Biosystems, Foster City, CA).

The proteins were expressed in *Escherichia coli* and purified from inclusion bodies as described previously for mIL-6 (*21*). The six N-terminal residues of each protein (Thr, Met, Ile, Thr, Asn, and Ser) are derived from β-galactosidase and the polylinker region of the pUC8 vector, with the remaining 162 residues corresponding to the sequence of mIL-6 beginning with Thr21.[2] Protein concentrations were determined by absorbance at 280 nm, where absorbancies of 1.05 and 1.1 correspond to concentrations of 1 mg/mL for ΔN22mIL-6 and Y78A, Y97A, and F173A, respectively, as determined by amino acid analysis (*22*).

Biological Assay. The hybridoma growth factor assay was performed as described previously (*23*). Briefly, IL-6-dependent 7TD1 cells were incubated in a 96-well microtiter plate (2000 cells/microwell), with serial dilutions of the test samples in a total volume of 0.2 mL. Cell growth was evaluated after 4 days at 37 °C by measuring hexosaminidase levels (*24*).

Nuclear Magnetic Resonance (NMR) Spectroscopy. Samples for NMR were prepared by dissolving lyophilized protein (usually 8−10 mg dry weight) in 500 μL of either ^2H_2O or 90% H_2O/10% ^2H_2O. ^1H NMR spectra were recorded on a Bruker AMX-600 spectrometer at a probe temperature of 20 °C. Solvent suppression was achieved by selective, low-power irradiation of the water resonance during the relaxation delay (typically, 1.5−1.8 s) and, in NOESY experiments, also during the mixing time. All two-dimensional spectra were recorded in the phase-sensitive mode using the time-proportional phase incrementation method (*25*). Two-dimensional NOESY spectra (*26, 27*) were recorded with a mixing time of 140 ms. Typically, 400−500 t_1 increments were acquired, with 160−176 scans and 4K data points per increment. Sweep widths were 7143 Hz for samples in H_2O and 6757 Hz for samples in ^2H_2O. One-dimensional spectra were acquired over 8K data points. Spectra were processed and analyzed on Silicon Graphics workstations using XWIN-NMR (version 1.3, from Bruker). Before Fourier transformation, phase-shifted (50−70°), sine-squared window functions were applied to two-dimensional spectra, and Lorentzian-to-Gaussian window functions were applied to one-dimensional spectra.

[2] Numbering throughout the text is that based on the hIL-6 sequence and the sequence alignment used in Simpson et al. (*3*). Thus, the first residue in natural mIL-6 (*22*) is Phe(−3).

Spectroscopic Measurements. Fluorescence data were collected on a Perkin-Elmer LS5 luminescence spectrophotometer using 0.5 cm path length cells at 25 °C and 5 nm slit widths. For intrinsic fluorescence, the excitation wavelength was 295 nm and the emission was monitored from 330 to 370 nm. For ANS fluorescence, the excitation wavelength was 350 nm and the emission was monitored from 450 to 530 nm. Circular dichroism measurements were performed using an Aviv (Lakewood, NJ) model 62DS CD spectrometer. All spectra are reported in terms of mean residue ellipticity $[\Theta]_{MRW}$. Far-UV CD spectra were recorded using a 0.1 cm path length cell with protein concentrations of 0.1 mg/mL, using an averaging time of 2 s, a bandwidth of 1 nm, and a step size of 1 nm. Reported spectra are the average of three scans with baseline subtractions. Estimates of secondary structural content were made using the reference spectra of ref *28* and a multilinear regression program (Prosec) supplied by Aviv. Near-UV spectra were recorded using a 1 cm path length cell with protein concentrations of 1 mg/mL, using an averaging time of 10 s, a bandwidth of 0.5 nm, and a step size of 0.2 nm. Reported spectra are baseline corrected.

Equilibrium Unfolding Experiments. Urea-induced unfolding of F173A and ΔN22mIL-6 was monitored by changes in the far-UV CD signal at 222 nm or Trp fluorescence λ_{max} as a function of urea concentration. The buffer that was used consisted of 20 mM sodium acetate (pH 4.0), and protein concentrations were 0.1 mg/mL. Samples were incubated at 25 °C for at least 30 min or at 37 °C for at least 15 min prior to measurement, and readings were taken only when the signal was stable. Alternate samples were measured in ascending and descending order, respectively, to avoid systematic error. The reversibility of unfolding was determined by diluting stock solutions of protein in 6 or 8 M urea into lower concentrations of denaturant. Data were analyzed with eq 1, which assumes a two-state unfolding transition and is based on equations by Santoro and Bolen (*29*) and Clarke and Fersht (*30*).

$$S = [(S_N - a[D] + S_U - b[D])\exp(A)]/[1 + \exp(A)] \quad (1)$$

where $A = m([D] - [D]_{50\%})/RT$, S is the measured property of the protein at a given denaturant (D) concentration, S_N is the signal of the native state, S_U is the signal of the denatured state, m is the slope of the curve in the transition region, R is the gas constant, and T is the absolute temperature, while a and b are the slopes of the pre- and post-transition baselines, respectively.

Thermal unfolding experiments were performed by measuring the far-UV CD signal at 222 nm (a protein concentration of 0.1 mg/mL and a path length of 0.1 cm) and the near-UV CD signal at 271 nm for F173A and at 281 nm for ΔN22mIL-6 (protein concentrations of 1.0 and 0.5 mg/mL, respectively, and a path length of 1.0 cm). The rate of heating was controlled by a peltier temperature controller in steps of 2 or 5 °C, with a signal integration time of 15 s.

Sedimentation Equilibria. Sedimentation experiments were performed on a Beckmann XL-A analytical ultracentrifuge equipped with absorption optics, using an An60-Ti rotor with cells containing quartz windows and Epon centerpieces. Equilibrium distributions were acquired at 16 000, 20 000, and 30 000 rpm in 0.001 cm radial increments and averaged

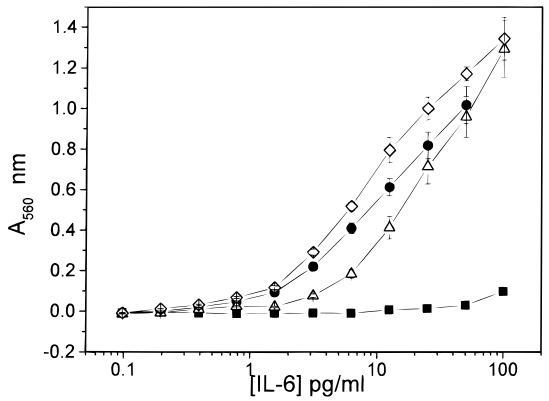

FIGURE 1: The biological activity of F173A is dramatically reduced over that of its parent protein ΔN22-mIL-6. Varying concentrations (0−100 pg/mL) of ΔN22mIL-6 (●), F173A (■), Y78A (△), and Y97A (◇) were incubated with 7TD1 cells for 4 days at 37 °C. The extent of cell proliferation was assessed as described in Materials and Methods. The experiment was performed in triplicate and was corrected for cell growth in the absence of IL-6.

over 10 measurements, and then fitted using the program WinNonLin, version 1.03 (Beckmann Instruments, Fullerton, CA). The partial specific volume of F173A (0.742 cm^3/g) and solution densities were calculated using the program SEDNTERP (*31*).

Limited Proteolysis. Proteins were subjected to proteolysis by pepsin and thermolysin (both from Boehringer Mannheim, Mannheim, Germany) at the following enzyme:substrate ratios: pepsin 1:100 at pH 2.0 and 1:10 at pH 4.0; thermolysin, 1:10 at pH 7.4 and 1:10 at pH 9. The buffers that were used were 20 mM glycine at pH 2.0, sodium acetate at pH 4.0, and phosphate at pH 7.4 and 9.0. Identical concentrations (0.1 mg/mL) of F173A and ΔN22mIL-6 were used to allow a direct comparison of their susceptibility to proteolysis. Proteolysis was allowed to proceed for the indicated periods of time in triplicate samples, whereupon aliquots were taken and the reactions stopped by the addition of NaOH (final concentration of 50 mM) for pepsin. Duplicate samples of each aliquot were analyzed by reverse phase high-performance liquid chromatography using a 2.1 mm × 100 mm Brownlee RP-100 column (Applied Biosystems) on an HP1090A liquid chromatograph (Hewlett-Packard) utilizing a TFA (0.1%)/acetonitrile (60%) gradient (buffer A being 0.1% TFA, and buffer B being 60% acetonitrile/0.089% TFA). The extent of proteolysis in each aliquot was determined by the extent of disappearance of the parent protein peak relative to the total protein content (area under the curve) of the chromatogram.

RESULTS

Biological Activity. ΔN22mIL-6, Y78A, Y97A, and F173A were expressed and purified to homogeneity, and their biological activities were determined by a mitogenic assay on murine 7TD1 cells (Figure 1). Y97A is marginally more and Y78A marginally less active than ΔN22mIL-6, while F173A is essentially devoid of activity, showing only a minimal response at the highest concentration that was tested (100 pg/mL).

F173A Has Native-like Secondary but a Reduced Level of Tertiary Structure. Detailed characterization of mIL-6 proteins was performed at pH 4.0, under low-salt conditions, rather than at pH 7.4 (which lies close to the isoelectric point) so the tendency to aggregate could be overcome (*32*−*34*). Far-UV CD and Trp fluorescence were used initially as indicators of secondary and tertiary structure, respectively. The Trp fluorescence emission intensity was slightly higher for F173A, but the wavelength maximum (λ_{max}) of both proteins was 345 nm. Both proteins exhibit the characteristic far-UV CD spectra of α-helical proteins with double minima at 208 and 222 nm (Figure 2A). The slightly lower signal of F173A corresponds to an estimated α-helical content of 42% compared with 59% for ΔN22mIL-6, 57% for Y78A, and 56% for Y97A (Table 1). At 37 °C, the temperature of the biological assay and the helical contents of F173A and ΔN22mIL-6 were essentially unchanged at 41 and 58%, respectively.

Table 1: Midpoints of Urea-Induced Denaturation of ΔN22mIL-6 and Mutants[a]

		$[urea]_{50\%}$[b] (M)	
protein	detection method	25 °C	37 °C
ΔN22mIL-6	fluorescence[c] λ_{max}	4.6 ± 0.1	4.6 ± 0.1
	far-UV[d] CD_{222}	4.6 ± 0.1	4.5 ± 0.3
F173A	fluorescence[c] λ_{max}	3.5 ± 0.3	3.5 ± 0.3
	far-UV[d] CD_{222}	2.6 ± 0.1	2.6 ± 0.3
Y78A	far-UV[d] $CD_{222\ nm}$	4.46 ± 0.05	−
Y97A	far-UV[d] $CD_{222\ nm}$	4.10 ± 0.05	−

[a] Solutions were equilibrated for at least 1 h prior to measurement. The buffer used in all cases was 20 mM sodium acetate (pH 4.0). Protein concentrations were 0.1 mg/mL. [b] Midpoints of urea denaturation ($[urea]_{50\%}$) were obtained by fitting eq 1 to equilibrium unfolding data. [c] Fluorescence measurements were made using a path length of 0.5 cm and excitation and emission slit widths of 5 nm. An excitation wavelength of 295 nm was used, and the emission wavelength maximum in the range 310−370 nm was determined. [d] The far-UV CD signal at 222 nm was monitored using a path length of 0.1 cm and the average of four measurements, each with a 10 s integration time.

The near-UV CD spectra of ΔN22mIL-6 and F173A were also compared (Figure 2B). While ΔN22mIL-6 exhibits a minimum at 281 nm and a maximum at 254 nm, which are characteristic of mIL-6 (*34*), these features are absent and reduced, respectively, for F173A. Because near-UV CD reports on tertiary structure from contributions of the aromatic residues, the loss of the signal in Figure 2B might be explained in part by the loss of a contributing Phe side chain. However, this could only constitute a small fraction of this signal loss as the protein contains a further nine aromatic residues (two Phe, five Tyr, and two Trp residues).

F173A Appears To Be Unfolded by NMR Spectroscopy. High-resolution ^1H NMR spectroscopy is a sensitive monitor of tertiary structure in proteins, and has been used previously with mIL-6 to identify interactions involving aromatic residues (*32*, *35*). The chemical shifts of the N-terminally truncated mIL-6 used in this study are essentially identical to those of Morton et al. (*17*), emphasizing the insensitivity of the bulk of the structure to deletion of the 22 N-terminal residues.

For Y78A, the chemical shifts of most well-resolved resonances are within 0.05 ppm of corresponding values in mIL-6 (Figure 3), indicating that the overall conformation of the protein is not significantly affected by substitution at this position. The spectrum of Y97A (Figure 3C) shows more significant chemical shift differences from that of mIL-6 but is still consistent with a correctly folded structure. Indeed,

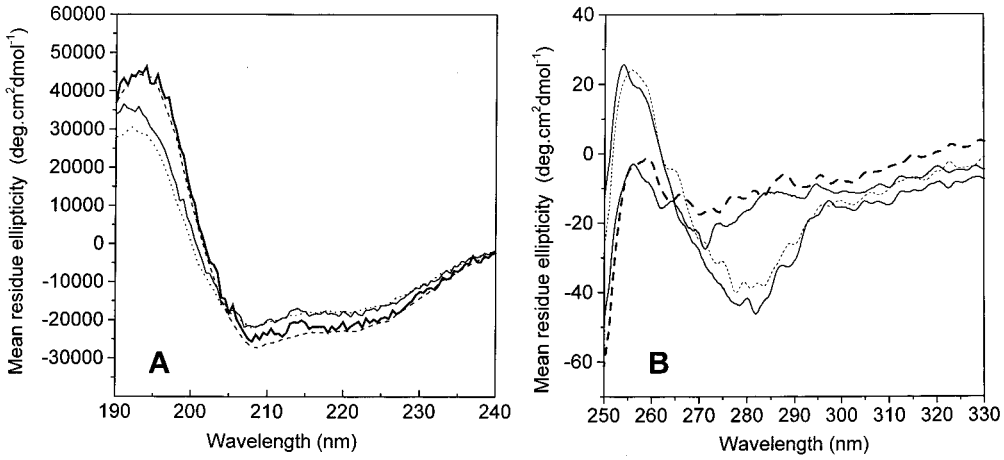

FIGURE 2: Circular dichroism spectra of ΔN22mIL-6 and F173A at 25 and 37 °C. (A) Far-UV CD spectra were recorded from 190 to 240 nm at 25 and 37 °C, using protein concentrations of 0.1 mg/mL and a path length of 1 mm, a step size of 1 nm, and an integration time of 2 s. Spectra are the average of three scans with buffer baseline correction. The buffer used in all cases was 20 mM sodium acetate (pH 4.0). For both panels: ΔN22mIL-6 at 25 °C (bold line) and 37 °C (dashed line) and F173A at 25 °C (solid line) and at 37 °C (dotted line). (B) Near-UV CD spectra were recorded from 250 to 330 nm at 25 and 37 °C, using protein concentrations of 1 mg/mL and a path length of 10 mm, a step size of 0.2 nm, and an integration time of 10 s. All spectra are buffer baseline corrected and have been subjected to adjacent averaging for increased clarity.

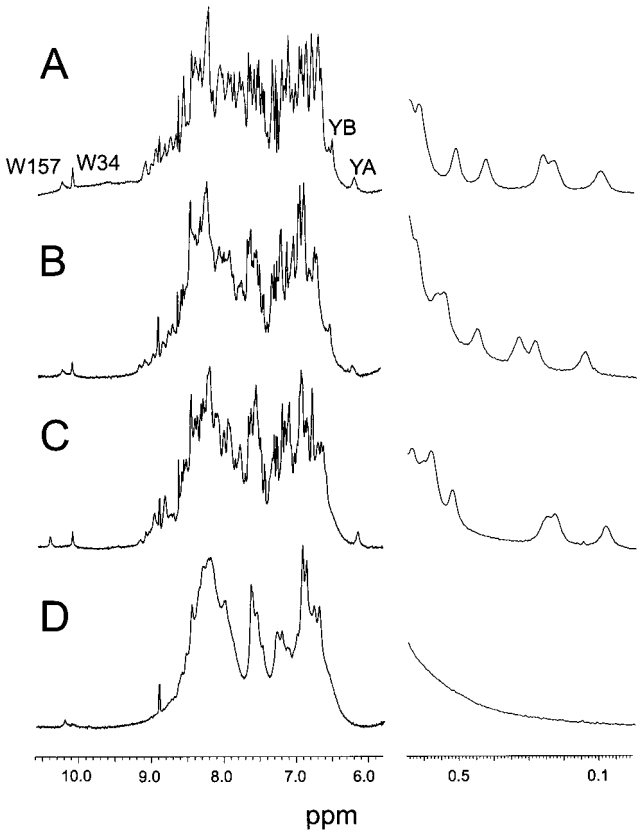

FIGURE 3: One-dimensional ^{1}H NMR spectra of ΔN22mIL-6, Y78A, Y97A, and F173A: (A) ΔN22mIL-6, (B) Y78A, (C) Y97A, and (D) F173A. Spectra were recorded at 600 MHz in 90% H_2O/10% ^2H_2O (pH 3.5, 20 °C). Left-hand panels show the aromatic and amide regions, and right-hand panels show the upfield methyl regions. Vertical scales are different in each case. The indole NH resonances of Trp34 and Trp157 are labeled. Note that the Y97A mutation caused either the loss of, or a significant shift in the position of, the C(3,5)H resonance of TyrB. As the C(3,5)H resonance of Y97A in hIL-6 occurs at almost exactly the same chemical shift as that of TyrB in mIL-6, it may be concluded that TyrB in mIL-6 corresponds to Y97 and that the loss of this resonance in Y97A is a direct result of mutation.

some shifts are in the direction of greater divergence from random coil values; for example, the indole NH resonance of W157, at 10.26 ppm in mIL-6, has moved further downfield.

These relatively small chemical shift differences stand in marked contrast to the spectrum of F173A (Figure 3D), which lacks the chemical shift dispersion and fine structure characteristic of a folded protein. A two-dimensional NOESY spectrum (not shown) confirms the lack of native-like tertiary interactions in F173A, but the lack of peak dispersion makes it impossible to ascertain if the sequential and medium-range NOEs characteristic of residual helical structure are still present.

The line widths in the one-dimensional spectrum of F173A (Figure 3D) are broader than those in the other mutants. Nevertheless, resolved resonances are still visible from the Trp indole NH and His C(2)H protons (near 10 and 9 ppm, respectively), indicating that the absence of upfield-shifted peaks in the aliphatic region is not due simply to broad line widths. Broad line widths can be an indication of aggregation. To determine if this was the case for F173A, we recorded one-dimensional spectra on a sample of F173A under identical conditions but at 1 mg/mL (50 μM; data not shown), where independent techniques (see below) have shown that F173A does not aggregate. This spectrum was slightly sharper than that shown in Figure 3D, but neither was as sharp as those of the other mutants (recorded at the higher concentration used for Figure 3) or as sharp as one would expect for a random coil protein. The lack of dispersion was still apparent. It is likely, therefore, that the broader line widths in Figure 3D arise partly from aggregation and partly from conformational averaging on a millisecond time scale in this protein.

F173A Preferentially Binds ANS but Is Not Susceptible to Proteolysis. The molten globule state (*36*) was originally defined theoretically as lying on the folding pathway of all proteins, with properties being intermediate between that of the folded and unfolded states. The term is now more commonly used to describe partially folded proteins which contain high levels of secondary structure and little tertiary structure. Another indicator of such states is the ability to bind the extrinsic hydrophobic fluorescence probe, ANS,

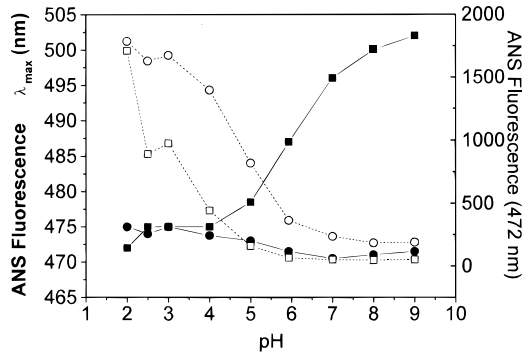

FIGURE 4: Binding of ANS. Fluorescence of ANS (excitation wavelength of 350 nm) in terms of wavelength maximum (left-hand abscissa) of ΔN22mIL-6 (□) and F173A (○) and emission intensity at 345 nm (right-hand abscissa) of ΔN22mIL-6 (■) and F173A (●) as a function of pH. Protein concentrations were 0.1 mg/mL; the path length was 5 mm, and slit widths were 5 nm. The buffers that were used were 20 mM glycine at pH 2.0, 2.5, and 3.0, 20 mM acetate at pH 4.0, 5.0, and 6.0, and 20 mM phosphate at pH 7.0, 8.0, and 9.0. Measurements were performed at 25 °C.

eliciting a dramatic blue shift of the intrinsic λ_{max} of ANS and a concomitant increase in its fluorescence emission intensity. In the presence of F173A, ANS has a blue-shifted λ_{max} over the pH range 2−9 (Figure 4), but in the presence of ΔN22mIL-6, this blue shift is only observed at or below pH 4 with a markedly reduced (30%) emission intensity.

The expanded structure of a molten globule state might be considered more susceptible to proteolytic cleavage. To determine if this was the case for F173A, F173A and ΔN22mIL-6 were subjected to partial proteolysis (Figure 5). At pH 4.0, there were no significant differences between the mutant and parent protein in their susceptibility to pepsin at 25 and 37 °C. At pH 7.4, the two proteins exhibited a slightly larger difference in their susceptibility to thermolysin at 25 °C, with ∼50% more proteolysis of F173A. Only at pH 2.0 and 9.0 was F173A dramatically more susceptible to pepsin and thermolysin, respectively.

F173A Lacks the Cooperative Unfolding of ΔN22mIL-6. F173A and ΔN22mIL-6 were subjected to equilibrium unfolding studies to determine their thermostabilities. Urea denaturation monitored by far-UV CD and Trp fluorescence emission λ_{max} (Figure 6A,B) is reversible for both proteins, as judged by the superimposition of unfolding and refolding curves, and data were essentially identical when the experiments were performed at 25 or 37 °C. Equation 1 was fitted to the combined data for unfolding and refolding at each temperature for each monitoring method, and the resultant values of $[urea]_{50\%}$ are shown in Table 1. For ΔN22mIL-6, the unfolding curves of both monitoring methods have a monophasic unfolding transition with a $[urea]_{50\%}$ of 4.6 ± 0.1 M, suggesting that the unfolding is essentially two-state, consistent with previous unfolding experiments on mIL-6 (*33*). The unfolding curves of both monitoring methods for F173A also exhibit monophasic unfolding transitions (Figure 6B), but they do not superimpose, the CD-monitored data yielding a $[urea]_{50\%}$ of 2.6 ± 0.1 M and the fluorescence λ_{max} data yielding a $[urea]_{50\%}$ of 3.5 ± 0.3 M. This suggests that the unfolding of F173A is not cooperative, and that the protein is significantly less stable than ΔN22mIL-6. Because the unfolding data for F173A had relatively short pretransition baselines, which can affect results of fitting, these data were additionally analyzed using both a fixed and a floated (but nonsloping) pretransition baseline. In all cases, the estimated $[urea]_{50\%}$ fell within the limits described above.

Y78A and Y97A were also subjected to urea-mediated equilibrium denaturation, monitored only by the far-UV CD signal at 222 nm, and the resultant values of $[urea]_{50\%}$ were 0.14 and 0.5 M lower than that of ΔN22mIL-6 (Table 1).

The Thermal Unfolding of both F173A and ΔN22mIL-6 Is Noncooperative. F173A and ΔN22mIL-6 were also subjected to thermal denaturation, being monitored by both far-UV CD (222 nm) and near-UV CD (271 nm for F173A and 281 nm for ΔN22mIL-6). These signals were monitored

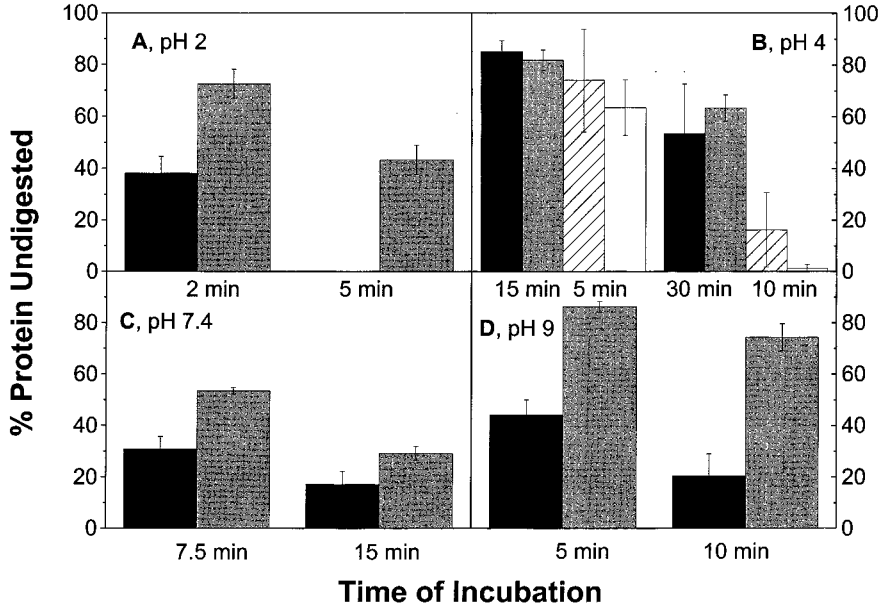

FIGURE 5: Effect of pH on the limited proteolysis of F173A and ΔN22mIL-6. The limited proteolysis of F173A (black columns) and ΔN22mIL-6 (gray columns) at 25 °C by (A) pepsin (1:100 enzyme-to-substrate ratio) in 20 mM glycine at pH 2, (B) pepsin (1:10 enzyme-to-substrate ratio) in 20 mM sodium acetate at pH 4, (C) thermolysin (1:10 enzyme-to-substrate ratio) in 20 mM phosphate buffer at pH 7.4, and (D) thermolysin (1:10 enzyme-to-substrate ratio) in 20 mM phosphate buffer at pH 9. Also, F173A (striped columns) and ΔN22mIL-6 (white columns) at 37 °C in 20 mM sodium acetate at pH 4. Protein concentrations were 0.1 mg/mL. Duplicate measurements on at least two separate samples were made for each time point.

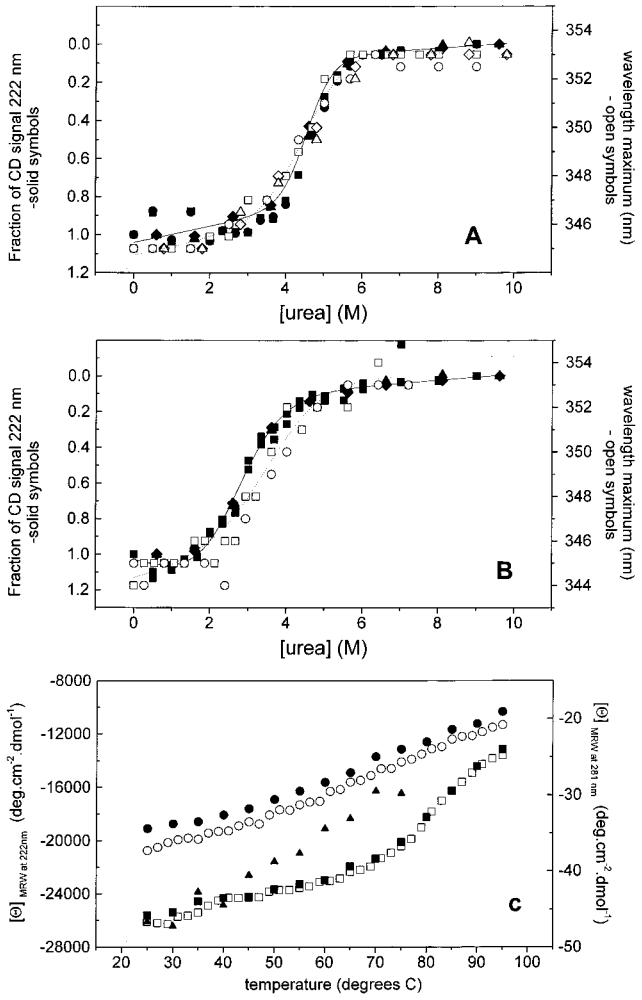

FIGURE 6: Equilibrium unfolding of F173A and ΔN22mIL-6. The urea-induced equilibrium unfolding of ΔN22mIL-6 (A) and F173A (B) were monitored by the fraction of CD signal at 222 nm (left-hand abscissa, black symbols) and by the emission λ_{max} of intrinsic Trp fluorescence in the range 310−370 nm (right-hand abscissa, white symbols). Unfolding at 25 (squares) and 37 °C (circles) and refolding at 25 (diamonds) and 37 °C (triangles) are shown. The lines shown are the fit of eq 1 to the combined unfolding and refolding data at 25 °C for CD (—) and fluorescence (···). The thermal unfolding of ΔN22mIL-6 and F173A was monitored by CD (C). Near-UV CD monitored unfolding of ΔN22mIL-6 at 281 nm (▲) using 5 °C heating increments. Far-UV CD monitored unfolding at 222 nm for both F173 (circles) and ΔN22mIL-6 (squares) using both 5 (black symbols) and 2 °C (white symbols) heating increments. The protein concentrations were 1 mg/mL for the near-UV CD experiment and 0.1 mg/mL for far-UV experiments, with 20 mM sodium acetate buffer at pH 4.0 used in all cases.

from 25 to 95 °C at two different heating rates (Figure 6C). In all cases, the unfolding was not reversible, as judged by a reduced signal intensity on cooling (data not shown). When the signal at 222 nm is monitored, ΔN22mIL-6 exhibits a slow loss of signal until approximately 70 °C, after which it appears to undergo a major unfolding transition (the midpoint of denaturation cannot be determined accurately because a post-transition baseline could not be achieved). In contrast, F173A exhibits only a slow loss of signal throughout the entire range of temperatures that were studied. When a faster rate of heating was used, the signal had a consistently lower magnitude, suggesting that the protein was more prone to aggregation under these conditions. When thermal unfolding was monitored by the near-UV signal, ΔN22mIL-6 and

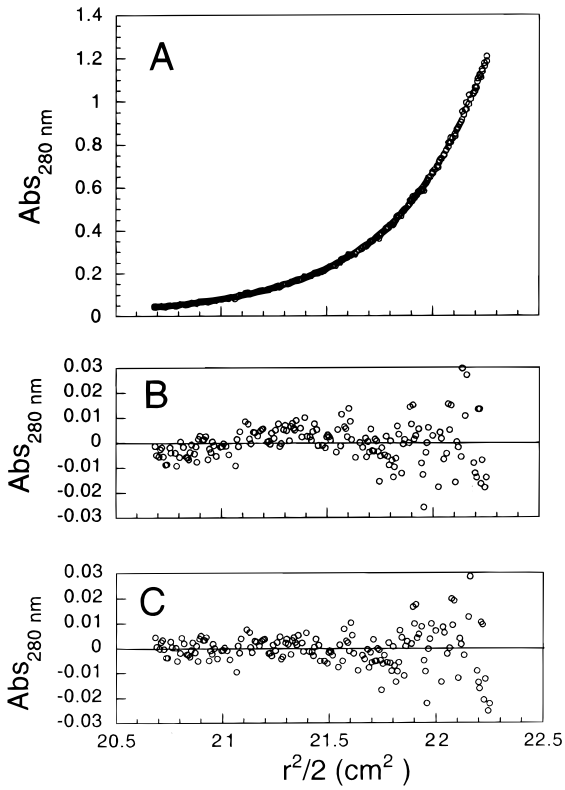

FIGURE 7: Sedimentation equilibrium indicates a monomer−dimer equilibrium. Panel A shows F173A at equilibrium at 30 000 rpm at a loading concentration of 0.3 mg/mL in 20 mM acetate buffer at pH 4.0. Panel B shows the residuals of a single-species equation fit to the data. Panel C shows the residuals of a monomer−dimer equilibrium equation fit to the data.

F173A exhibited steady losses of signal intensity until 70 and 45 °C, respectively. Beyond these temperatures, the magnitude of the signal increases, apparently due to the aggregation of the proteins at the 10-fold increase in protein concentrations required for near-UV CD experiments. More dilute solutions in longer path length cells could not be used to overcome these problems for this experiment because the larger sample volumes do not allow efficient heating.

Oligomerization and Aggregation States of F173A. Given the tendency of mIL-6 to aggregate under various conditions, several observations, such as line broadening in NMR spectra and protection against proteases, might have resulted from the increased level of aggregation of F173A. To address this issue, the concentration dependence of fluorescence was assessed at pH 4.0 in 20 mM acetate buffer. No such dependence was observed over the concentration range 0.01−1 mg/mL, nor were any changes observed for a 0.1 mg/mL solution of F173A over a time period of 24 h. However, the addition of 150 mM NaCl resulted in a marked increase in fluorescence intensity and a concomitant blue shift of λ_{max}. The oligomerization state of F173A was also assessed by sedimentation equilibrium analysis using a range of loading concentrations (0.1−1 mg/mL) in 20 mM sodium acetate (pH 4.0). The data fit best to a monomer ↔ dimer model (Figure 7) with an association constant of 2.9×10^3 M^{-1}. Recombinant hIL-6 tends to form a metastable dimer under some conditions which is indistinguishable from the human IL-6 monomer in many ways, including susceptibility to proteolytic cleavage (*37*). Thus, it seems unlikely that the low-affinity F173A monomer ↔ dimer equilibrium affects

the interpretation of our results. When the same experiments were performed in the presence of 150 mM NaCl, F173A formed very large aggregates which sedimented at low speeds.

DISCUSSION

Mutational methods for identifying active sites of proteins, such as alanine scanning, often require that large numbers of mutant proteins be produced and screened for biological and/or binding activities. It can be demanding in terms of time and resources to produce the milligram quantities of protein required for rigorous structural analyses. Fortunately, many biological assays require only small quantities of each protein, and equivalent activities are an excellent indicator that structural integrity has been preserved in mutant proteins. However, while the absence or reduction of activity may indicate that an active site residue has been identified, it could also mean that the structure of the protein has been perturbed, even in the case of mutations to alanine, which are generally assumed to be nonperturbing.

In this study, two aromatic to alanine mutations were shown to have very little effect on the activity of ΔN22mIL-6, and the subsequent characterization of these proteins confirmed that they were native-like. In contrast, the mutation of a single phenylalanine residue at position 173 resulted in the loss of biological activity, initially suggesting that Phe173 might play a role in the formation of the mIL-6−IL-6R−gp130 complex. We have shown, however, that, although this possibility could not be fully discounted, structural perturbation of F173A is a much more likely cause of this loss of activity.

Far-UV CD and intrinsic tryptophan fluorescence, which are commonly used as probes of secondary and tertiary structure, respectively, and which require comparatively low quantities of protein, suggested that F173A was native-like. It was only the use of more discriminating probes of tertiary structure, specifically near-UV CD and ^{1}H NMR, that revealed a lack of tertiary structure in this protein. These spectral properties, and several other characteristics, such as an enhanced ability to bind ANS, noncooperative unfolding, and an enhanced tendency to aggregate at concentrations of >1 mg/mL, all suggest that F173A is molten globule-like. To date, there are relatively few reports of single mutations causing the formation of molten globule states, although one notable exception is bovine pancreatic phospholipase A_2, in which many different mutations induce molten globule-like states (*38*, and references therein). The number of proteins for which this is true, however, is likely to increase as more mutant proteins are characterized structurally.

Because proteases only cleave flexible regions of polypeptide chains, loosened conformations should be more prone to proteolytic attack. Indeed, this is a method which has been used to probe the structure of partially folded states (*39*) and, in combination with bacteriophage systems, to select stable proteins (*40*). However, at pH 4.0, where F173A is molten globule-like, it is no more susceptible to proteolysis than its parent protein. This confirms observations made by De Filippis et al. (*41*), who proposed that the molten globule-like state of an hIL-6 variant, lacking 22 N-terminal residues and one of two disulfide bonds due to the double mutation C44S/C50S, was protease resistant at low pH. Where that study compared the proteolysis of different proteins, this study compared the susceptibility of two forms of the same protein that differ by only one residue, but where F173A is molten globule-like. This resistance to proteolysis could simply be a property pertaining to the four-α-helix bundle topology of IL-6; however, previous studies of partially folded states showed that they were susceptible to proteolysis at only one or two sites (*39*). Thus, high levels of secondary structure may be enough to confer a reasonable level of proteolytic stability for other protein folds. Thus, although limited proteolysis can be a powerful probe of structure, it may not be a universal measure of native-like structure and should be used with care.

The fluorescence data for F173A present apparently contradictory views of the tertiary structure of this mutant. On one hand, although the tryptophan fluorescence of F173A is native-like, both near-UV and NMR data clearly show that the protein lacks the well-defined tertiary structure of the parent protein. On the other hand, the midpoint of unfolding detected by far-UV CD precedes that obtained by fluorescence. If fluorescence were a good probe of tertiary structure, then this second observation suggests that the loss of secondary structure precedes the loss of tertiary structure, which runs counter to commonly accepted mechanisms of protein denaturation. However, the first observation, that native-like levels of fluorescence are observed in the absence (or at least vastly reduced levels) of tertiary structure, points to the fact that tryptophan fluorescence is not a good indicator of global tertiary structure for F173A. In mIL-6, Trp fluorescence at pH 4.0 stems mainly from Trp157, with little contribution from Trp34, which is quenched below pH 7 by the charged side chain of His31 (*37*). It is not practical to further probe the unfolding of any residual tertiary structure in F173A by near-UV CD because of the weak signals observed using this technique.

Thus, it appears that the unfolding transitions of F173A must relate to the unfolding of the α-helices and some residual tertiary contacts in the vicinity of the Trp residues, which must be quite stable despite a dramatic reduction in the level of tertiary structure. This was also observed for partially unfolded disulfide-modified variants of mIL-6 (*34*). It should also be noted that the unfolding of ΔN22mIL-6 may also hinge on the stability of the α-helical structure. Thermally unfolded ΔN22mIL-6 exhibits an unfolding transition above 70 °C by far-UV CD but a gradual loss of signal by near-UV CD to near baseline levels at 70 °C. These data suggest that the tertiary structure of mIL-6 is marginally stable, but that the four-helix bundle structure, even if imperfectly packed or molten globule-like, is very thermostable.

This may also be the case for several other four-α-helix bundle cytokines. Several members of this family are domain-swapped, a process which is thought to occur when proteins are partially unfolded but maintain high levels of secondary structure (*42*). For example, hIL-6 undergoes dimer dissociation at low levels of denaturant but where it maintains native-like levels of helix (*37*). Granulocyte colony-stimulating factor appears to unfold partially at low pH, but maintains a high level of secondary structure (*43*). Having marginally stable tertiary structure but a stable global fold may be important in terms of protein evolution for this class of structurally and functionally related cytokines, which

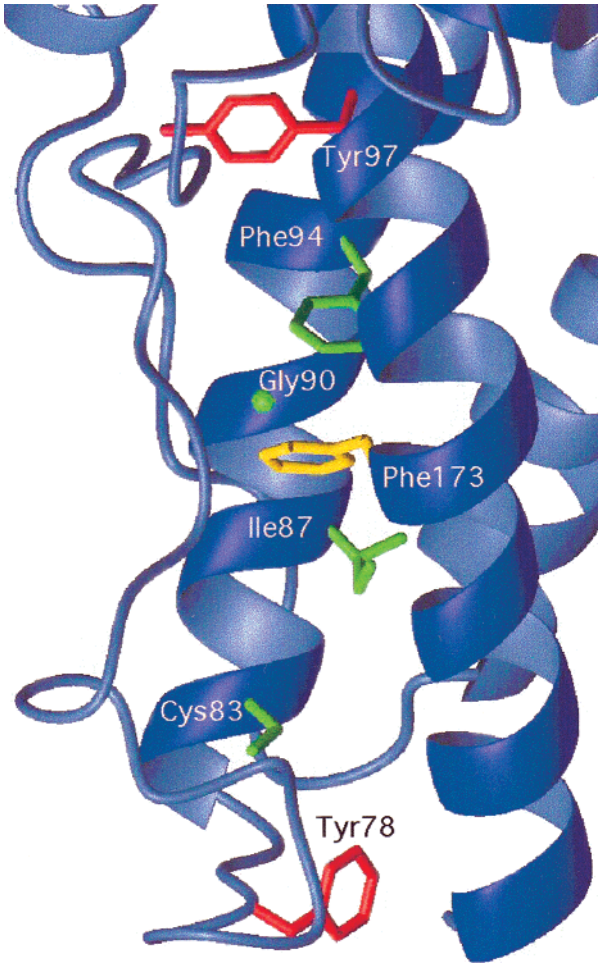

FIGURE 8: Position of Phe173 and residues with which it makes NOE contact. The side chain of Phe173 is colored yellow, while the side chains of Cys83, Ile87, Gly90, and Phe94 are colored green. The side chains of Tyr97 and Tyr78 (Phe78 in human IL-6) are colored red. The structure was created using MolMol from coordinates of the solution structure of human IL-6 [PDB file 2il6 (*11*)].

comprises a number of different subgroups. Many locally destabilizing amino acid substitutions could be tolerated because of the thermodynamic and proteolytic stability of the overall helical fold. It should be noted, however, that tertiary structure within this fold can be very stable. For example, leukemia inhibitory factor maintains its tertiary structure over a wide range of pH and temperature conditions and exhibits very slow amide exchange (*44*−*46*).

The molten globule-like properties of F173A were determined in vitro on the isolated protein. It is possible that binding to the IL-6 receptor might induce a more stable (and less molten globule-like) structure in this mutant protein and that Phe173 could still play an important role in activity. However, inspection of the high-resolution structure of hIL-6 (*10*, *11*) suggests that possibility is unlikely as Phe173 appears to be a key structural residue, rather than a potential binding site. Phe173 is fully conserved in 15 mammalian species as well as in a viral homologue of IL-6 (*47*), and many of the residues with which it makes contact are highly conserved. Phe173 lies in helix D and makes interhelical nuclear Overhauser effect (NOE) contacts with four residues in helix B, Cys83, Ile87, Gly90, and Phe94 (Figure 8; *20*). Mutation to alanine is likely to remove one or more interactions that are critical for the packing of helices B and D, and therefore for stabilizing tertiary structure in general.

In contrast, Tyr97, which is located on helix B and also plays a role in the packing of helices B and D, appears to be involved in fewer interactions. Tyr78, which is located in loop B−C, does not appear to make significant interactions with the rest of the protein. Consequently, mutation to alanine at these positions merely has the effect of slightly destabilizing the protein without disrupting the overall tertiary structure.

A previous study on the same F173A mutation in hIL-6 (F173AhIL-6) showed that this protein contained high levels of α-helix and was recognized by a neutralizing IL-6 antibody, but had reduced levels of IL-6 receptor binding (as determined by cell-binding experiments), and very low levels of biological activity (*48*). As such, Phe173 was interpreted as forming part of receptor binding site 1, which binds to the IL-6R and comprises residues in loop A−B, the N-terminus of helix B, and the C-terminus of helix D. In light of our results for mIL-6, it seems more likely that F173AhIL-6 has structural perturbations similar to that of F173A. Several other mutations in this region which resulted in the loss of activity of hIL-6 (*49*, *50*) but involved residues that are not solvent-exposed may also cause structural perturbations. To our knowledge, the structures of these mutant proteins have not been fully characterized.

In conclusion, it can been seen that the single mutation F173A in mIL-6 results in the loss of biological activity in the protein. This loss of activity is interpreted as resulting from a global disruption of the tertiary structure of the protein, and not from the substitution of an important residue in receptor binding site 1. While the fine structure of the protein has been lost, high levels of secondary structure are maintained and the conformation resembles that of a molten globule which is resistant to proteolysis.

ACKNOWLEDGMENT

We thank R. L. Moritz for providing purified protein and A. W. Burgess for critical comment on the manuscript.

REFERENCES

1. Akira, S., Taga, T., and Kishimoto, T. (1993) *Adv. Immunol. 54*, 1−78.
2. Narazaki, M., and Kishimoto, T. (1994) in *Guidebook to cytokines and their receptors* (Nicola, N., Ed.) pp 56−58, Oxford University Press, Oxford, U.K.
3. Simpson, R. J., Hammacher, A., Smith, D. K., Matthews, J. M., and Ward, L. D. (1997) *Protein Sci. 6*, 929−955.
4. Hirano, T. (1994) in *The Cytokine Handbook*, 2nd ed. (Thompson, A., Ed.) pp 145−167, Academic Press, San Diego, CA.
5. Hallek, M., Bergsagel, P. L., and Anderson, K. C. (1998) *Blood 91*, 3−21.
6. Rettig, M. B., Ma, H. J., Vesico, R. A., Põld, M., Schiller, G., Belson, D., Savage, A., Nishikubo, C., Wu, C., Fraser, J., Said, J. W., and Berenson, J. R. (1997) *Science 276*, 1851−1857.
7. Hibi, M., Murakami, M., Saito, M., Hirano, T., Taga, T., and Kishimoto, T. (1990) *Cell 63*, 1140−1157.
8. Ward, L. D., Howlett, G. J., Discolo, G., Yasukawa, K., Hammacher, A., Moritz, R. L., and Simpson, R. J. (1994) *J. Biol. Chem. 269*, 23286−23289.
9. Paonessa, G., Graziani, R., de Serio, A., Savino, R., Ciapponi, L., Lahm, A., Salvati, A. L., Toniatti, C., and Ciliberto, G. (1995) *EMBO J. 14*, 1942.

10. Somers, W., Stahl, M., and Seehra, J. S. (1997) *EMBO J. 16*, 989−997.
11. Xu, G. Y., Yu, H. A., Hong, J., Stahl, M., McDonagh, T., Kay, L. E., and Cumming, D. A. (1997) *J. Mol. Biol. 268*, 468−481.
12. Bravo, J., Staunton, D., Heath, J. K., and Jones, E. J. (1998) *EMBO J. 17*, 1665−1674.
13. Lowe, D. M., Winter, G., and Fersht, A. R. (1987) *Biochemistry 26*, 6038−6043.
14. Cunningham, B. C., and Wells, J. A. (1989) *Science 244*, 6841−6847.
15. Blaber, M., Baase, W. A., Gassner, N., and Matthews, B. W. (1995) *J. Mol. Biol. 246*, 317−330.
16. Hammacher, A., Reid, G. E., Moritz, R. L., and Simpson, R. J. (1997) *Biomed. Chromatogr. 11*, 337−342.
17. Morton, C. J., Bai, H., Zhang, J.-G., Hammacher, A., Norton, R. S., Simpson, R. J., and Mabbutt, B. C. (1995) *Biochim. Biophys. Acta 1249*, 189−203.
18. Proudfoot, A. E. I., Brown, S. C., Bernard, A. R., Bonnefoy, J.-Y., and Kawashima, E. H. (1993) *J. Protein Chem. 12*, 489−497.
19. Nishimura, C., Watanabe, A., Gouda, H., Shimada, I., and Arata, Y. (1996) *Biochemistry 35*, 273−281.
20. Xu, G.-Y., Hong, J., McDonagh, T., Stahl, M., Kay, L. E., Seehra, J., and Cumming, D. A. (1996) *J. Biomol. NMR 8*, 123−135.
21. Zhang, J.-G., Moritz, R. L., Reid, G. E., Ward, L. D., and Simpson, R. J. (1992) *Eur. J. Biochem. 207*, 903−913.
22. Simpson, R. J., Moritz, R. L., Nice, E. C., Grego, B., Yoshizaki, F., Sugimura, Y., Freeman, H., and Murata, M. (1986) *Eur. J. Biochem. 157*, 497−506.
23. Van Snick, J., Cayphas, S., Vink, A., Uyttenhove, C., Coulie, P., Rubira, M. R., and Simpson, R. J. (1986) *Proc. Natl. Acad. Sci. U.S.A. 89*, 10998−11001.
24. Landegran, U. (1984) *J. Immunol. Methods 67*, 379−388.
25. Marion, D., and Wüthrich, K. (1983) *Biochem. Biophys. Res. Commun. 113*, 967−974.
26. Anil Kumar, Ernst, R. R., and Wüthrich, K. (1980) *Biochem. Biophys. Res. Commun. 95*, 1−6.
27. Macura, S., Huang, Y., Suter, D., and Ernst, R. R. (1981) *J. Magn. Reson. 43*, 259−281.
28. Yang, J. T., Wu, C.-S. C., and Martinez, H. M. (1986) *Methods Enzymol. 130*, 208−296.
29. Santoro, M. M., and Bolen, D. W. (1988) *Biochemistry 27*, 8063−8068.
30. Clarke, J., and Fersht, A. R. (1993) *Biochemistry 32*, 4322−4329.
31. Laue, T. M., Shah, B. D., Ridgeway, T. M., and Pelletier, S. L. (1992) in *Ananlytical Ultracentrifugation in Biochemistry and Polymer Science* (Harding, S. E., Rowe, A., and Horton, J. C., Ed.) pp 90−125, Cambridge, U.K.
32. Matthews, J. M., Ward, L. D., Hammacher, A., Norton, R. S., and Simpson, R. J. (1997) *Biochemistry 36*, 6187−6189.
33. Ward, L. D., Matthews, J. M., Zhang, J. G., and Simpson, R. J. (1995) *Biochemistry 34*, 11652−11659.
34. Zhang, J.-G., Matthews, J. M., Ward, L. D., and Simpson, R. J. (1997) *Biochemistry 36*, 2380−2389.
35. Ward, L. D., Hammacher, A., Zhang, J.-G., Weinstock, J., Yasukawa, K., Morton, C. J., Norton, R. S., and Simpson, R. J. (1993) *Protein Sci. 2*, 1472−1481.
36. Ptitsyn, O. B. (1992) in *Protein Folding* (Creighton, T. E., Ed.) pp 234−300, W. H. Freeman and Co., New York.
37. Matthews, J. M., Hammacher, A., Howlett, G. J., and Simpson, R. J. (1998) *Biochemistry 37*, 10671−10680.
38. Yuan, C., Byeon, I.-J. L., Poi, M.-J., and Tsai, M.-D. (1999) *Biochemistry 38*, 2919−2929.
39. Fontana, A., Polverino de Laurento, P., De Fillipis, V., Scaramella, E., and Zambonin, M. (1997) *Folding Des. 2*, R17−R26.
40. Kristensen, P., and Winter, G. (1998) *Folding Des. 3*, 321−328.
41. De Filippis, V., Polverino de Laurento, P., Toniutti, N., and Fontana, A. (1996) *Biochemistry 35*, 11503−11511.
42. Bennett, M. J., Schlunegger, M. P., and Eisenberg, D. (1995) *Protein Sci. 4*, 2455−2468.
43. Kolvenbach, C. G., Nahri, L. O., Philo, J. S., Li, T., Zhang, M., and Arakawa, T. (1997) *J. Pept. Res. 50*, 310−318.
44. Maurer, T., Smith, D. K., Owczarek, C. M., Layton, M. J., Zhang, J. G., Nicola, N. A., and Norton, R. S. (1994) *Growth Factors 11*, 271−276.
45. Hinds, M. G., Maurer, T., Zhang, J. G., Nicola, N. A., and Norton, R. S. (1997) *J. Biomol. NMR 9*, 113−126.
46. Purvis, D. H., and Mabbutt, B. C. (1997) *Biochemistry 36*, 10146−10154.
47. Moore, P. S., Boshoff, C., Weiss, R. A., and Chang, Y. (1996) *Science 274*, 1739−1744.
48. Li, X., Rock, F., Chong, P., Cockle, S., Keating, A., Ziltner, H., and Klein, M. (1993) *J. Biol. Chem. 268*, 22377−22384.
49. Nishimura, C., Kutatsugi, K., Yasukawa, K., Kishimoto, T., and Arata, Y. (1991) *FEBS Lett. 311*, 167−169.
50. Nishimura, C., Ekida, T., Nomura, K., Sakamoto, K., Suzuki, H., Yasukawa, K., Kishimoto, T., and Arata, Y. (1992) *FEBS Lett. 311*, 271−275.

BI991973I